

ating range of the impeller airflow rate and the flow parameters at the impeller exit, formulating quality criteria as airflow-averaged impeller power characteristics, and searching for advisable values of the impeller blade geometric parameters by systematically scanning the independent-variable region at points that form a uniformly distributed sequence. The numerical investigation conducted showed that the proposed technique offers a sizeable increase in the compression ratio of a centrifugal impeller while keeping its adiabatic efficiency within the operating range of the impeller airflow rate. This conclusion was made when using rather a "coarse" computational grid, which, however, retains the sensitivity of the computed results to a variation in the centrifugal impeller blade shape. This conclusion was verified by a subsequent calculation of the power characteristics of the original and the modified impeller on a finer grid. On the whole, it was shown that varying the shape of the middle part of a centrifugal impeller blade alone has a pronounced effect on the impeller compression ratio, while leaving the impeller adiabatic efficiency almost unaffected. The results obtained may be used in the aerodynamic optimization of centrifugal stages of aircraft gas turbine engines.

, : , -
 , , -
 , , . -
 -
 -
 -
 [4, 5], [1], [2, 3] -
 -
 -
 , -
 -
 , -
 . -
 : -
 , -
 -
 -
 [6]. -
 , -
 . -
 1. -
 (-
). -
 . -
 2. , -
 . -
 3. -
 . -
 , -

(k - ε) -

$$\frac{\partial \rho}{\partial \tau} + \text{div} (\rho \vec{V}) = 0, \quad (1)$$

$$\frac{\partial}{\partial \tau} (\rho v^i) + \text{div} (\rho \vec{V} v^i) = \text{div} (\mu \text{grad } v^i) + S^i, \quad i=1,2,3, \quad (2)$$

$$\frac{\partial}{\partial \tau} (\rho E) + \text{div} (\rho \vec{V} E) = \text{div} \left(\frac{\kappa}{C_v} \text{grad } E \right) + S_c^E, \quad (3)$$

$$\frac{\partial}{\partial \tau} (\rho k) + \text{div} (\rho \vec{V} k) = \text{div} (\mu_{ef.k} \text{grad } k) + G - \rho \varepsilon, \quad (4)$$

$$\frac{\partial}{\partial \tau} (\rho \varepsilon) + \text{div} (\rho \vec{V} \varepsilon) = \text{div} (\mu_{ef.\varepsilon} \text{grad } \varepsilon) + C_1 \frac{\varepsilon}{k} G - C_2 \rho \frac{\varepsilon^2}{k}, \quad (5)$$

$$S^i = -g^{i\alpha} \frac{\partial}{\partial q^\alpha} \left(\rho + \frac{2}{3} \rho k \right) + \frac{1}{\Delta} \frac{\partial}{\partial q^\alpha} \left\{ \Delta \left[\lambda g^{i\alpha} \frac{1}{\Delta} \frac{\partial}{\partial q^j} (\Delta v^j) + \mu \left(g^{i\beta} \frac{\partial v^\alpha}{\partial q^\beta} + v^n g^{i\beta} \Gamma_{n\beta}^\alpha + v^n g^{\alpha\gamma} \Gamma_{n\gamma}^i \right) \right] \right\} - \Gamma_{\beta\alpha}^i (\rho v^\beta v^\alpha + \tilde{p}^{\beta\alpha}) + F^i;$$

$$\tilde{p}^{\delta\alpha} = -\lambda g^{\delta\alpha} \frac{1}{\Delta} \frac{\partial}{\partial q^j} (\Delta v^j) - \mu \left[g^{\delta\beta} \frac{\partial v^\alpha}{\partial q^\beta} + g^{\alpha\gamma} \frac{\partial v^\delta}{\partial q^\gamma} + v^n (g^{\delta\beta} \Gamma_{n\beta}^\alpha + g^{\alpha\gamma} \Gamma_{n\gamma}^\delta) \right];$$

$$S_c^E = -\frac{1}{\Delta} \frac{\partial}{\partial q^\alpha} \left\{ \Delta \left[v^\beta g_{n\beta} (\rho g^{n\alpha} + \tilde{p}^{n\alpha}) + \frac{\kappa}{C_v} g^{\alpha\beta} \frac{\partial (V^2/2)}{\partial q^\beta} \right] \right\} + \vec{V} \cdot \vec{F};$$

$$G = \mu_t \left[g_{\alpha\gamma} \left(\frac{\partial v^\gamma}{\partial q^\beta} + \Gamma_{\beta\rho}^\gamma v^\rho \right) \right] \times \left[g^{\beta n} \frac{\partial v^\alpha}{\partial q^n} + g^{\alpha l} \frac{\partial v^\beta}{\partial q^l} + v^m (g^{\beta n} \Gamma_{mn}^\alpha + g^{\alpha l} \Gamma_{ml}^\beta) \right];$$

v^j - ; \tilde{V} ; τ - ;
 ρ - ; p - ; μ - (-
) ; $\lambda = -2\mu/3$; F^i -

$$\begin{aligned}
 q^j & - \bar{F} (\quad); \\
 & ; g_{\delta\gamma} - \quad ; \Delta = \sqrt{\det \|g_{\delta\gamma}\|} ; \\
 \Gamma_{\eta\gamma}^\delta & - \quad ; E = C_V T + V^2 / 2 (C_V - \quad); \\
 k \quad \varepsilon & - \quad , T - \quad ; \kappa - \quad ; \\
 \mu_{ef.k} = \mu_t & \quad (\mu_t - \quad); \mu_{ef.\varepsilon} = \mu_t / 1,3; C_1 = \\
 1,44; C_2 & = 1,92.
 \end{aligned}$$

(1) – (5)

MLU [7].

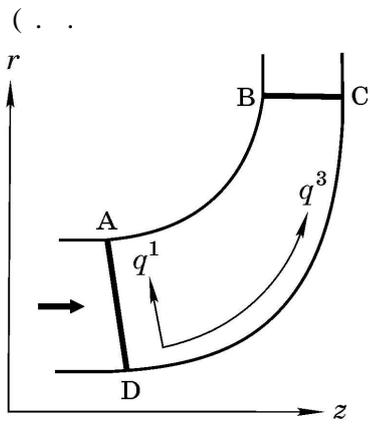
(1) – (5)

(2), (4) (5)
(1), (3) –

$$\Delta = \sqrt{\det \|g_{\delta\gamma}\|} .$$

$$\Delta \rho v^3 (\quad , \quad)$$

, [8, 9].



.1

ABCD

$q^1, q^2, q^3,$

$r \quad z$

$q^1 \quad q^3.$

$q^1 \quad q^3,$

.1

AD BC

DC

AB

$q^2,$

$\tilde{\varphi}(q^1, q^3),$

$\tilde{\varphi} -$

$q^2,$

$q^1 \quad q^3,$

$q_h^1 \quad q_s^1$

$q^1,$

(.1).

$q_l^3 \quad q_t^3$

$q^3,$

$\tilde{\varphi}(q^1, q^3)$

q^1

$\varphi(q^3).$

q_{l1}^3

$q_l^3 \leq q^3 \leq q_{l1}^3$ (

$q_{l1}^3 \leq q^3 \leq q_t^3).$

q^1

$q_h^1 \leq q^1 \leq q_s^1$

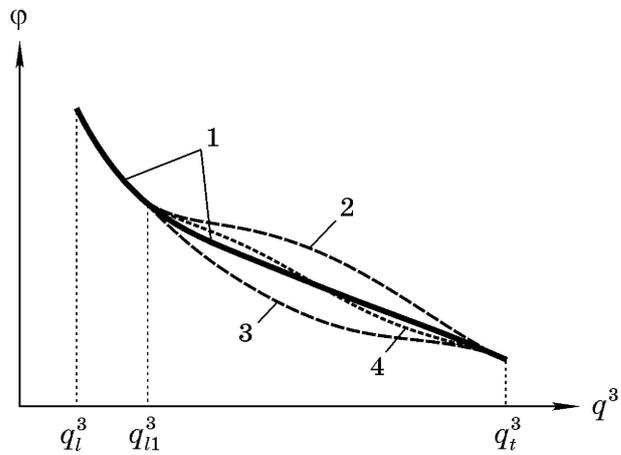
$$\varphi^*(q^3) = f(q^3) - \varphi(q^3),$$

(6)

$$\varphi(q^3) - \dots$$

$$1 \dots 2; f(q^3) - \dots$$

$$f(q^3) = \varphi(q_{l1}^3) + [\varphi(q_t^3) - \varphi(q_{l1}^3)] \left(\frac{q^3 - q_{l1}^3}{q_t^3 - q_{l1}^3} \right)^2. \quad (7)$$



. 2

$$\varphi^*(q^3) \dots (6) \dots (7) \dots q_{l1}^3 \dots q_t^3$$

$$\varphi_v^*(q^3) = \varphi^*(q^3) [1 + y_B(q^3)], \quad (8)$$

$$y_B(q^3) - \dots (q^3 - \dots)$$

P_0, P_1, P_2, P_3

$$P_0(q_{l1}^3, 0), P_1[q_{l1}^3 + 0,3(q_t^3 - q_{l1}^3), y_1], P_2[q_{l1}^3 + 0,7(q_t^3 - q_{l1}^3), y_2], P_3(q_t^3, 0), \quad (9)$$

$$y_1 \dots y_2 - \dots \varphi_n(q^3),$$

$$\varphi_n(q^3) = f(q^3) - \varphi_v^*(q^3). \quad (10)$$

(6) - (10)

$$y_2 < 0; \dots y_1 > 0, y_2 > 0; \dots y_1 < 0,$$

$$y_1 < 0, y_2 > 0. \dots$$

(6) – (10)

$d\varphi/dq^3$ -

$q_{l1}^3 \quad q_t^3$.

$y_1 \quad y_2$

$$y_1 = 2y_m(\xi_1 - 0,5), \quad (11)$$

$$y_2 = 2y_m(\xi_2 - 0,5), \quad (12)$$

y_m - ; (ξ_1, ξ_2) - -

[10].

($\pi_{p.k.}^*$) $\eta_{p.k.}^*$

$\pi_{p.k.}^*$.

$$\hat{\eta}_{p.k.}^* = \frac{2}{G_{\max} - G_{\min}} \int_{G_{\min}}^{\frac{G_{\min} + G_{\max}}{2}} \eta_{p.k.}^* dG, \quad \hat{\pi}_{p.k.}^* = \frac{2}{G_{\max} - G_{\min}} \int_{G_{\min}}^{\frac{G_{\min} + G_{\max}}{2}} \pi_{p.k.}^* dG, \quad (13)$$

(G_{\min}, G_{\max}) -

$12 \times 12 \times 72$ (

[11].

16

(11), (12)

$y_m = 0,7$.

. 3,

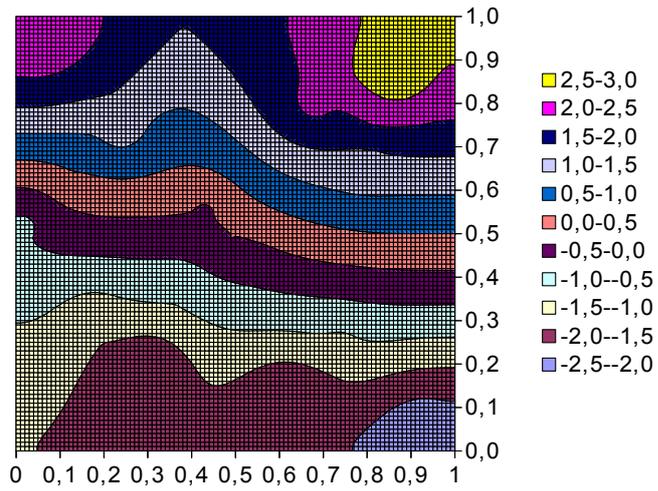
ξ_1

ξ_2

$\hat{\pi}_{p.k.}^*$

16

[12].



. 3

$\hat{\eta}_{p.k.}^*$

0,3 %

. 3

(0,063;0,938)

16

$\hat{\pi}_{p.k.}^*$

:

2,3 % ($\hat{\eta}_{p.k.}^*$

0,1 %);

(0,875;0,875)

$\hat{\pi}_{p.k.}^*$

2,8 % ($\hat{\eta}_{p.k.}^*$

0,3 %).

4 . 2, -

3.

(
20 × 20 × 120

. 4

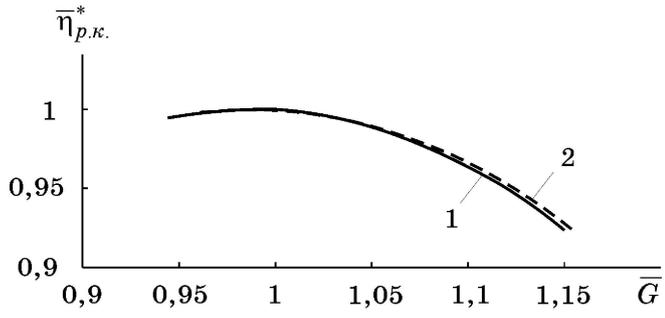
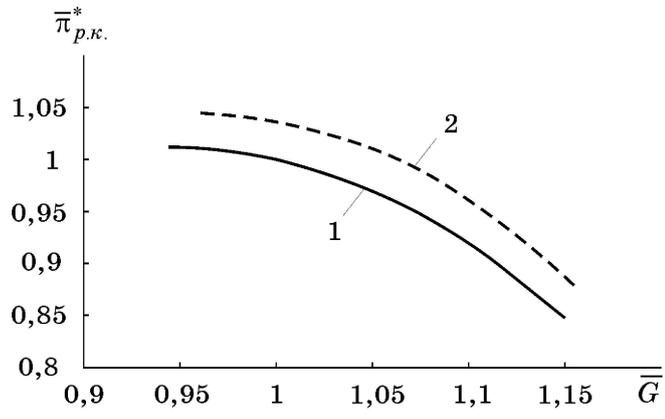
(2)

(1)

$\bar{\pi}_{p.k.}^*$, $\bar{\eta}_{p.k.}^*$ \bar{G} .

(13)

3,2 %,



. 4

1. Benini E., Giacometti S. Design, manufacturing and operation of a small turbojet-engine for research purposes. Applied Energy. 2007. Vol. 84. P. 1102–1116.

2. 2018. . 20. 2. . 43–54.

